

JERZY KAMIENSKI, ANDRZEJ DUDA<sup>1</sup>

## ON THE LIQUID FLOW RATES IN DUAL MIXING VESSEL IN CONTEXT OF COMPARTMENT MODEL APPROACH

### PRZEPIŁYWY CIECZY W MIESZALNIKU Z DWOMA MIESZADŁAMI W KONTEKŚCIE OBSZAROWEGO MODELU MIESZANIA

#### Abstract

The study was dedicated to the question of pumping and circulation flow rates of liquid in the dual mixing vessel. When the two impellers have different geometries, one of them is always predominant imposing the structure and rate of the total liquid flow in the vessel. In case the flow structure is multi-loop, the overall liquid flow is then equal to circulation flow rate increased by the additional inter-stage flow rates, appearing between neighbouring loops. This feature can be described with usage of Compartment Model Approach (CMA).

*Keywords: dual mixing vessel, flow rate, CMA model*

#### Streszczenie

Pracę poświęcono zagadnieniu przepływów cieczy w zbiornikach z dwoma mieszadłami, odnoszących się do bezpośredniego obszaru mieszadeł jak też do całej przestrzeni zbiornika. Jeśli mieszadła posiadają różną geometrię, jedno z nich jest zawsze mieszadłem dominującym, decydującym o globalnym przepływie cieczy. W przypadku struktury w zbiorniku złożonej z kilku pętli krążącej cieczy, na całkowity przepływ, oprócz tych w graniach każdej z pętli, składają się dodatkowe przepływy występujące między sąsiadującymi pętlami, co można opisać wykorzystując do tego model CMA.

*Słowa kluczowe: mieszanie, dwa mieszadła, przepływ cieczy, model CMA*

<sup>1</sup> Prof. dr hab. inż. Jerzy Kamiński, mgr inż. Andrzej Duda, Politechnika Krakowska.

## 1. Introduction

The apparatuses equipped with two or more impellers i.e. dual or multi mixing vessels are often found in industrial installations. They seem to be an alternative versus standard constructions with single impeller, especially for mixing applications in bigger liquid volumes. The slender vessels, in which the height greatly exceeds their diameter and the shape factor is over unit, are then usually applied. Those vessels are equipped with two or more impellers assembled on the shaft.

The magnitudes describing liquid flow in the dual mixing vessels are ones of those technical key-issues that influence the selection of the impeller's geometry as well as the vessel itself. The intensity and structure of the flows relate to the mixing time required to gain the final effects of the process progressing within [1]. Those magnitudes depend on the geometry of used impellers, their position in vessel, as well as on the rotational speed and vessel's design. The liquid flow rate related to the mixing power determines efficiency, which is one of the basic criteria of the mixing vessel applicability [2, 3, 4]. Until recently, the pumping flow rate  $Q_p$  has been commonly recognised as a basic value used for description of the liquid flow in the mixing vessel [5]. However, it is believed for a few years that the flow rate should be evaluated in the total vessels' volume, as the additional flows entrained by the impellers' discharge and circling around the local centres of formed liquid loops are included in calculation [3, 4, 6]. Therefore, it was proposed to introduce the circulation flow rate  $Q_c$  as the basic magnitude characterising the impellers' functioning.

The flow structure in the dual mixing vessels can form one single circulation loop or be more complex and consist of the number of interacting loops. The exchange phenomena of the kinetic energy in the liquid occurs, as a result of the inter-stage flow rate  $Q_E$ , being induced by the fluctuation of an axial component of velocity [7, 8]. In this case, the  $Q_c$  flow rate is understand as the sum of the flow rates evaluated in each loop, increased by the total value of the  $Q_E$  flows found on the all borders of the interaction between loops [9].

The inter-correlations of the magnitudes describing liquid flows in the mixing vessel, verified by the selected examples of the dual impeller configurations, were presented in the paper.

## 2. The experimental data and set-up

The liquid flow rates were evaluated by the integration of the mean and fluctuating velocity profiles in vessel, normal or parallel to its axis. The liquid velocity values were measured using laser anemometry technique LDA. The cylindrical vessel with diameter  $D = 0.286$  m was equipped with two impellers. The used impellers had different geometries and constant diameter  $d = 0.095$  m and were put together creating different configurations. The geometry and dimensions of the impellers used were described in the paper [10]. The impeller spacing  $\Delta h$  was varied within the range of  $(0.5 \div 2) d$  however, the lower impeller clearance was constant,  $0.5 \cdot d$ . The measurements were carried out at constant rotational speed,  $5 \text{ s}^{-1}$ . The vessel was filled with working liquid – dimethyl sulfoxide (DMSO) up to a height (H) of  $1.5 \cdot D$ . The liquid viscosity was of  $2.3 \text{ mPas}$ . The description of the experimental set-up as well as the measurement methods of the liquid velocities were

presented in the papers [9, 10]. Furthermore, the evaluation algorithm of the flow rates  $Q$  was described in [9, 11, 12].

### 3. The pumping flow rate

The pumping flow rate is commonly determined by the rate of the volumetric flow that enters  $Q_{in}$  or leaves  $Q_{out}$  the zone swept by rotating impeller, i.e. the flow rate passing across the planes established by rotating blades of the impeller, similarly to the rotating pump case [3, 5]:

$$|Q_p| = |Q_m| = |Q_{out}| \quad (1)$$

where each of the above flow rates is calculated on the base of mean velocity components, normal to the  $A_S$  plane established by rotating impeller:

$$Q_{in(out)} = \int_{A_S} \bar{u}_{n, in(out)} dA_S \quad (2)$$

In practice, more universal and often used is the dimensionless pumping flow number  $K_p$  [ $1 \div 8$ ]:

$$K_p = \frac{Q_p}{n \cdot d^3} \quad (3)$$

dependent only on the impeller's geometry in fully developed turbulent flow. The  $Q_p$  flow rate in the dual mixing vessels is the sum of the flows induced both by the upper ( $Q_{p up}$ ) and the lower ( $Q_{p low}$ ) impeller, regardless of their position in vessel [12]:

$$Q_{p sum} = Q_{p up} + Q_{p low} \quad (4)$$

Thus, the dimensionless pumping flow number  $K_p$  for the dual impeller with constant diameter assembled on common shaft, takes form:

$$K_{p sum} = K_{p up} + K_{p low} \quad (5)$$

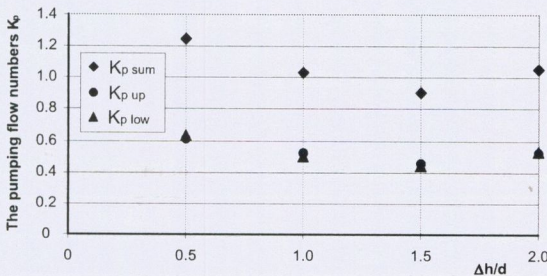


Fig. 1. The pumping flow numbers  $K_p$  for the set of two PBT-6/45° turbines

Rys. 1. Liczby pompowania  $K_p$  dla zestawu dwóch turbin PBT-6/45°

The  $K_p$  numbers for upper and lower impeller as well as its total values, versus impeller spacing  $\Delta h$  was shown on the following figures, exemplified by the case of two Pitched Blade Turbines PBT-6/45° (figure 1). Moreover, the  $K_p$  values were collected in table 1. It can be concluded from the graphs that for the investigated dual impellers with identical geometries, the  $K_{p\ up}$  and  $K_{p\ low}$  numbers take nearly similar values, independently the  $\Delta h$  spacing value. The dual impeller sets with identical geometries operate the same way, i.e. yield proportional variations of the induced flow rates. The  $K_p$  values reach local extrema at  $\Delta h = 1.5 \cdot d$ . It would point on mutual damping of the induced flows.

If the dual set consists of impellers with different geometries, one of them is always predominant. Thus, this impeller generates usually higher flow rates – yielding in higher  $K_p$  values, which has an influence on the  $K_{p\ sum}$  number variations versus impeller spacing  $\Delta h$  and has strong effect on the final structure of the flow field in the vessel.

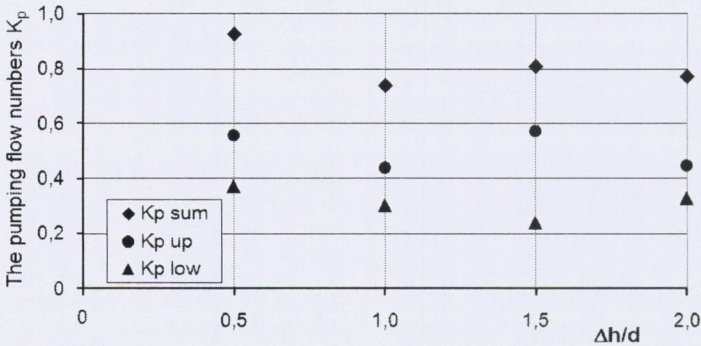


Fig. 2. The pumping flow numbers  $K_p$  for the impeller set: lower – hydrofoil Chemineer HE-3, upper – RT-6 turbine

Rys. 2. Liczby pompowania  $K_p$  dla zestawu: dolne mieszadło – hydrofoil Chemineer HE-3, górne mieszadło – turbina RT-6

This dependence is described on the graph, figure 2. It shows the dependence of the  $K_p$  numbers on the impeller spacing  $\Delta h$ , for the dual set: upper impeller – RT-6 turbine, lower – hydrofoil Chemineer HE-3. In this case the upper impeller is the predominant. The exact values of  $K_p$  numbers were collected in table 2.

Table 1

The  $K_{p\ sum}$ ,  $K_{p\ up}$  and  $K_{p\ low}$  values for the set of two PBT-6/45° turbines

| The pumping flow number | $\Delta h / d$ |      |      |      |
|-------------------------|----------------|------|------|------|
|                         | 0.5            | 1.0  | 1.5  | 2.0  |
| $K_{p\ sum}$            | 1.25           | 1.02 | 0.90 | 1.05 |
| $K_{p\ up}$             | 0.61           | 0.52 | 0.46 | 0.52 |
| $K_{p\ low}$            | 0.64           | 0.50 | 0.44 | 0.53 |

The  $K_{p\ sum}$ ,  $K_{p\ up}$  and  $K_{p\ low}$  values for the set of two impellers: lower – HE-3, upper – RT-6

| The pumping flow number | $\Delta h / d$ |      |      |      |
|-------------------------|----------------|------|------|------|
|                         | 0.5            | 1.0  | 1.5  | 2.0  |
| $K_{p\ sum}$            | 0.93           | 0.74 | 0.81 | 0.78 |
| $K_{p\ up}$             | 0.56           | 0.44 | 0.57 | 0.45 |
| $K_{p\ low}$            | 0.37           | 0.30 | 0.24 | 0.33 |

#### 4. The circulation flow rate

The circulation flow rate  $Q_c$  is defined as total value of the flow determined in any axial or radial profile of the vessel ( $r_i$ ), ( $z_i$ ) i.e. normal or parallel to its axis, on the base of mean velocity components ( $\bar{u}_r$ ,  $\bar{u}_z$ ) normal to the profile section ( $r_i$ ,  $z_i$ ) [3]:

$$Q_c = \max_r \{ |Q_r| \} = \max_z \{ |Q_z| \} \quad (6)$$

where:

$$Q_r(r_i) = 2 \cdot \pi \cdot r_i \cdot \int_{z_1}^{z_2} (\bar{u}_r)_{r_i} dz \quad (7)$$

$$Q_z(z_i) = 2 \cdot \pi \cdot \int_{r_1}^{r_2} (\bar{u}_z)_{z_i} \cdot r dr \quad (8)$$

Similarly to the pumping flow rate, the circulation flow rate  $Q_c$  is in practice determined by the dimensionless circulation flow number [3]:

$$K_c = \frac{Q_c}{n \cdot d^3} \quad (9)$$

which depends only on the impeller's geometry in fully developed turbulent flow. The mentioned geometry strongly corresponds to the structure of flow in the dual mixing vessel and can form one loop, circulating along the liquid height or can be composed of a number of interacting loops, figure 3. In first case, the  $Q_c$  flow rate is evaluated according to the equations (6), (7) i (8). However, when the complex structure of the flow is taken into consideration, the  $Q_c$  flow rate is the sum of the flow rates evaluated within borders of each of n-loops:

$$Q_c = \sum_{i=1}^n Q_{ci} \quad (10)$$

and thus:

$$K_c = \sum_{i=1}^n K_{ci} \quad (11)$$

In case of simple flow structure, consisting of the one single circulation loop, there is a lack of additional flows entrained by the impellers' discharge and circling around the local centres. As a result, the flow rate of liquid passing the impellers' region is nearly equal to the flow of liquid in the total volume of vessel. This correspondence was presented for the

case of two PBT-6/45° turbines. Figure 4 shows the collected  $K_{p\ sum}$  and  $K_c$  numbers versus four values of the impeller spacing  $\Delta h$  related to impeller diameter. The graphs depicted confirm the thesis mentioned above, with exception the spacing  $\Delta h = 1.5 \cdot d$ . Probably, it is an evidence for local disturbances in the flow structure, occurring at spacing value  $1.5 \cdot d$ . The values of the  $K_{p\ sum}$  and  $K_c$  numbers were confronted in table 3. The last right hand column includes proportional ratio of the  $K_c$  to  $K_{p\ sum}$ .

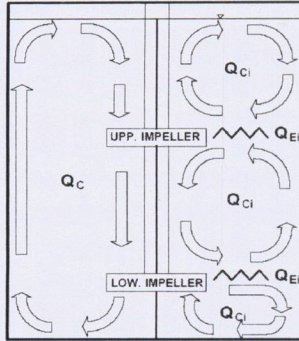


Fig. 3. The liquid flow structure in the dual mixing vessel. Left hand side: one loop circulating along the liquid height. Right hand side: the case of several loops

Rys. 3. Struktura przepływu cieczy w mieszalniku z dwoma mieszadłami. Lewa strona: jedna pętla cieczy krążącej wzdłuż wysokości w zbiornik. Prawa strona: kilka pętli cieczy

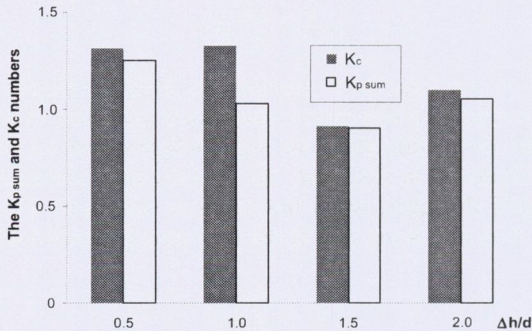


Fig. 4. The comparison of the pumping flow number  $K_p$  and the circulation flow number  $K_c$ , for the dual set of two PBT-6/45° turbines

Rys. 4. Porównanie liczby wydajności pompowania  $K_p$  oraz liczby wydajności przepływu w mieszalniku  $K_c$  na przykładzie zestawu dwóch turbin PBT-6/45°

If the flow structure consists of two or more loops, the local disturbances cause dynamic increase of the liquid flow rate in the vessel related to the flow rate through the impeller region.

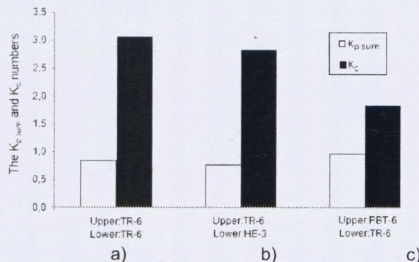


Fig. 5. The comparison of the pumping flow number  $K_p$  sum and the circulation flow number  $K_c$  for the three dual sets: a) two RT-6 turbines, b) upper impeller: RT-6 turbine, lower impeller: hydrofoil Chemineer HE-3, c) upper impeller: PBT-6/45° turbine, lower impeller: RT-6 turbine

Rys. 5. Porównanie liczby wydajności pompowania  $K_p$  oraz liczby wydajności przepływu w mieszalniku  $K_c$  na przykładzie trzech zestawów mieszadeł: a) dwie turbiny RT-6, b) górne mieszadło: turbina RT-6, dolne mieszadło: hydrofoil Chemineer HE-3, c) górne mieszadło: turbina PBT-6/45°, dolne mieszadło: turbina RT-6

Table 3

The confrontation of the  $K_c$  and  $K_{p\ sum}$  values for the set of two PBT-6/45° turbines

| $\Delta h / d$ | $K_c$ | $K_{p\ sum}$ | $K_c / K_{p\ sum}$ |
|----------------|-------|--------------|--------------------|
| 0.5            | 1.31  | 1.25         | 1.05               |
| 1.0            | 1.33  | 1.03         | 1.29               |
| 1.5            | 0.92  | 0.90         | 1.02               |
| 2.0            | 1.10  | 1.05         | 1.04               |

As the spacing  $\Delta h$  is enlarged, the quotient of  $K_c / K_{p\ sum}$  increases dynamically, reaching its extrema at  $\Delta h = 2 \cdot d$ . Then, the liquid flow rate in the total vessel exceeds nearly three times the flow rate within the impellers' region. As a result, in the geometrical conditions of the vessel and dual impellers presented above, there are strong liquid flows induced, which circulate outside the impeller regions and reinforce themselves mutually.

### 5. The inter-stage flow rates $Q_E$ . The CMA model

According to the state of the art, the exchange phenomena of the kinetic energy between respective liquid loops circulating in the vessel occurs as a result of the additional, inter-stage flow rate  $Q_E$ , [7, 8, 9, 13]. The flow  $Q_E$  is situated at the point of contact of the two neighbouring loops and is thought to be induced by the fluctuation of an axial component of velocity. Similarly to the  $Q_c$  and  $Q_p$  flow rates, the inter-stage flow rate is expressed in the dimensionless form [7, 13]:

$$K_E = \frac{Q_E}{n \cdot d^3} \quad (12)$$

If the flow structure in the vessel consists of a number of loops, the total inter-stage flow rate is then the sum of the  $Q_{Ei}$  flow rates, existing on the all interaction borders between respective loops. It also can be expressed as by the dimensionless criteria:

$$K_E = \sum_{i=1}^n K_{Ei} = \frac{\sum_{i=1}^n Q_{Ei}}{n \cdot d^3} \quad (13)$$

The total flow of the liquid in vessel is then caused both by the flows within each loop space,  $Q_{ci}$ , and the flows on the border,  $Q_{Ei}$ . The correlations between those magnitudes are described by the compartment model (CMA) [7, 8, 13]. The thorough study of the CMA model leads to the conclusion that the real total circulation flow rate  $Q_c$  in the dual mixing vessel, considering the equations (6) ÷ (9), should be in fact defined by the corrected formula:

$$Q_{c \text{ KOR}} = \sum_i Q_{ci} + \sum_i Q_{Ei} \quad (14)$$

and then:

$$K_{c \text{ KOR}} = \sum_{i=1}^n K_{ci} + \sum_{i=1}^n K_{Ei} = \frac{Q_{c \text{ KOR}}}{n \cdot d^3} \quad (15)$$

The corrected circulation flow rate  $Q_{c \text{ KOR}}$ , evaluated above, depends on the geometric parameters of the dual mixing vessel. In case of the simple flow structure (one loop):  $\sum Q_{Ei} = 0$ , and then  $Q_{c \text{ KOR}} \approx Q_c$ . When the complex flow structures are taken into consideration,  $Q_{c \text{ KOR}} > Q_c$ , as was presented in figure 7, exemplified by the impeller set: lower HE-3, upper RT-6. In order to make a comparison, the magnitude of  $K_{p \text{ sum}}$  was added to the graph. The numerical values were collected in table 4. The following graph illustrates the scale of a phenomenon – the difference between the  $K_{c \text{ KOR}}$  and  $K_{p \text{ sum}}$ . It proofs, in the cases of the complex flow structure and the geometry of impellers, that the real flow rates in the vessel are greatly higher than it seemed to result from the study of the pumping capacity exclusively for the impellers.

Table 4

**The confrontation of the  $K_{p \text{ sum}}$ ,  $K_c$  and  $K_{c \text{ KOR}}$  for the set of impellers: lower HE-3, upper RT-6**

| $\Delta h/d$ | $K_{p \text{ sum}}$ | $K_c$ | $K_{c \text{ KOR}}$ |
|--------------|---------------------|-------|---------------------|
| 0.5          | 0.93                | 2.15  | 3.00                |
| 1.0          | 0.74                | 1.93  | 3.59                |
| 1.5          | 0.81                | 3.08  | 3.98                |
| 2.0          | 0.78                | 2.83  | 3.88                |



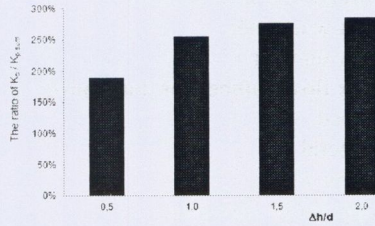
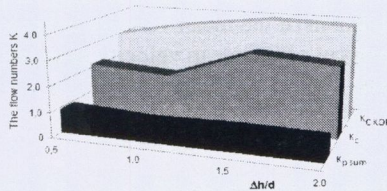


Fig. 6. The proportional ratio of  $K_c/K_{p\text{sum}}$  for the dual set: upper impeller: RT-6 turbine, lower impeller: hydrofoil A-315, versus different values of  $\Delta h/d$

Rys. 6. Wartości ułamka  $K_c/K_{p\text{sum}}$  dla zestawu dwóch mieszadeł: górne – turbina RT-6, dolne – hydrofoil A-315, w funkcji różnych wartości  $\Delta h/d$



Rys. 7. Porównanie  $K_{p\text{sum}}$ ,  $K_c$  oraz  $K_{C\text{KOR}}$  dla zestawu mieszadeł: dolne HE-3, górne RT-6, w funkcji różnych wartości  $\Delta h/d$

Fig. 7. The confrontation of the  $K_{p\text{sum}}$ ,  $K_c$  and  $K_{C\text{KOR}}$  for the impeller set: lower HE-3, upper RT-6, versus different values of  $\Delta h/d$

## 6. Resumé

The presented study pays attention to the aspect of the liquid flow rates in the dual mixing vessel. The knowledge of the flow structure and the flow rates is the key-issue, influencing the proper design of the vessel, impeller as well as the processes which are going to be conducted. The correct assumption of the flow rates, based on the corrected values of  $Q_{CKOR}$  and  $K_{CKOR}$ , assures the correct geometry and dimensions of the device, including the sufficient safety and reserve factor.

## Symbols

|            |                           |     |
|------------|---------------------------|-----|
| $D$        | – tank diameter           | [m] |
| $d$        | – impeller diameter       | [m] |
| $H$        | – liquid height           | [m] |
| $\Delta h$ | – impeller spacing        | [m] |
| $K$        | – flow number, general    | [–] |
| $K_c$      | – circulation flow number | [–] |

|             |   |                     |
|-------------|---|---------------------|
| $K_{C KOR}$ | – corrected circulation flow number                 | [–]                 |
| $K_E$       | – inter–stage flow number                           | [–]                 |
| $K_p$       | – pumping flow number                               | [–]                 |
| $K_{p sum}$ | – total pumping flow number for dual impeller       | [–]                 |
| $n$         | – rotational speed                                  | [s <sup>-1</sup> ]  |
| $Q$         | – flow rate, general                                | [m <sup>3</sup> /s] |
| $Q_c$       | – circulation flow rate                             | [m <sup>3</sup> /s] |
| $Q_{C KOR}$ | – corrected circulation flow rate                   | [m <sup>3</sup> /s] |
| $Q_E$       | – inter–stage flow rate                             | [m <sup>3</sup> /s] |
| $Q_p$       | – pumping flow rate                                 | [m <sup>3</sup> /s] |
| $Q_{p sum}$ | – total pumping flow rate for dual impeller         | [m <sup>3</sup> /s] |
| $Q_r$       | – maximal flow rate in radial profile               | [m <sup>3</sup> /s] |
| $Q_z$       | – maximal flow rate in axial profile                | [m <sup>3</sup> /s] |
| $r$         | – vessel’s radius                                   | [m]                 |
| $\bar{u}_n$ | – mean velocity component, normal to impeller plane | [m/s]               |
| $\bar{u}_r$ | – radial component of the mean velocity in vessel   | [m/s]               |
| $\bar{u}_z$ | – axial component of the mean velocity in vessel    | [m/s]               |
| $z$         | – vessel’s axis                                     | [m]                 |

### Literature

- [1] Nienow A. W.: *Chemical Engineering Science*, 52, (1997), 2557-2565.
- [2] Kamiński J.: *Mieszanie układów wielofazowych*, WNT, Warszawa 2004.
- [3] Jaworski Z., Nienow A. W., Dyster K. W.: *Canadian Journal of Chemical Engineering*, 74, (1996), 3-15.
- [4] Jaworski Z., Nienow A. W., Koutsakos E., Dyster K. W., Bujalski W.: *Trans IChemE, Part A*, 69, (1991), 313-320.
- [5] Stręk F.: *Mieszanie i mieszalniki*, WNT, Warszawa 1981.
- [6] Jaworski Z., Nienow A. W.: *Eighth European Conference on Mixing*, Cambridge, (1994), N<sup>o</sup> 136.
- [7] Vrábel P., van der Lans R. G. J. M., Luyben K. Ch. A. M., Boon L., Nienow A. W.: *Chemical Engineering Science*, 55, (2000), 5881-5896.
- [8] Vsconcelos J. M. T., Alves S. S., Barata J. M.: *Chemical Engineering Science*, 50, (1995), 2343-2354.
- [9] Duda A., Kamiński J., Talaga J.: *Inżynieria i Aparatura Chemiczna*, Nr 2, (2010), 27-28.
- [10] Duda A., Talaga J.: *16<sup>th</sup> International Conference “Chemical Engineering and Plant Design”*, Berlin 2006, 159-168.
- [11] Duda A., Kamiński J., Talaga J.: *Czasopismo Techniczne*, 5-M, (2008), (105), 67-78.
- [12] Duda A., Kamiński J., Talaga J.: *Czasopismo Techniczne*, 2-M, (2008), (105), 67-74.
- [13] Otomo N., Bujalski W., Nienow A. W.: *The 1995 IChemE Research Event / First European Conference*, (1995), 829-831.